Chemical Science

ROYAL SOCIETY OF CHEMISTRY

EDGE ARTICLE

Cite this: DOI: 10.1039/d4sc05920d

All publication charges for this article have been paid for by the Royal Society of Chemistry

In silico screening of *P,N*-ligands facilitates optimization of Au(III)-mediated *S*-arylation†

Joseph W. Treacy, James A. R. Tilden, Elaine Y. Chao, Zihuan Fu, Alexander M. Spokoyny,* K. N. Houk* and Heather D. Maynard*

Metal-mediated cysteine *S*-arylation is an emerging bioconjugation technique due to its high chemoselectivity, rapid kinetics, and aqueous compatibility. We have previously demonstrated that by altering the steric profile of the ligand and aryl groups of an Au(III) oxidative addition complex, one can modulate the kinetics of the bimolecular coordination and induce rate constants up to 16 600 M^{-1} s^{-1}. To further enhance the rate of coordination, density functional theory (DFT) calculations were performed to investigate the steric properties of the *P,N*-ligated Au(III) oxidative addition complex as well as the thermodynamics of the *S*-arylation reaction. This allowed for the accelerated screening of 13 new Au(III) oxidative addition complexes. Three of the more sterically available, synthetically accessible *P,N*-ligands were synthesized, incorporated into Au(I) and Au(III) complexes, and their rates determined experimentally. The comprehensive mechanistic insights from the DFT calculations led to the development of new reagents with bimolecular coordination rate constants as fast as 20 200 M^{-1} s^{-1}. Further experimental characterization of these reagents' efficacy as *S*-arylation reagents led to a proposed switch in selectivity-determining step for the fastest reagent, which was further confirmed by profiling the reductive elimination kinetics. This work provides a concise workflow for the screening of metal-mediated cysteine *S*-arylation reagents and new fundamental insights into the coordination chemistry behavior of Au(III) systems.

Received 3rd September 2024
Accepted 15th January 2025

DOI: 10.1039/d4sc05920d

rsc.li/chemical-science

Introduction

Effective bioconjugation reagents are chemoselective for specific residues, amenable to mild and aqueous reaction conditions, and able to perform reactions at low concentrations, which necessitates favorable reaction kinetics. Cysteine presents itself as a common target for site-selective bioconjugation due to its high nucleophilicity, relatively low abundance in the proteome, and ability to be incorporated into proteins, antibodies, and other biomolecules through molecular biology techniques.[1–3] Commonly used cysteine modifications rely on addition to maleimides or other Michael acceptors. However, these linkages are susceptible to retro-Michael reactions under reducing conditions, leading to reversible modification of the biomolecule.[4–9] Accordingly, cysteine *S*-arylation has emerged as a unique approach to produce C(sp^2)–S bonds, which are less susceptible to reversibility.[10] Many cysteine *S*-arylation approaches rely on nucleophilic aromatic substitution (S_NAr), which necessitates electron withdrawing groups *ortho* or *para* to a leaving group.[11–19] This limits the aryl substrate scope for potential modification. An alternative method uses metal-mediated or metal-catalyzed cysteine *S*-arylation, which allows for the *ex situ* or *in situ* formation of an oxidative addition complex (OAC).[20–30] These OACs are then able to permit initial thiol coordination to the metal center and subsequent reductive elimination to form the stable, C(sp^2)–S bond. The use of transition metals allows for the aryl scope to be broadly expanded to contain both electron donating and withdrawing substituents as well as different substitution patterns.

The *ex situ* formation of the OAC can provide a set of bench stable reagents that can be used for subsequent biomolecule transformations without any additional precautions to preserve the metal reagent.[31,32] By using thiophilic metal centers (*e.g.* Pd and Au), exquisite chemoselectivity for thiols and rapid kinetics are observed. Notably, the mechanism for the *S*-arylation proceeds *via* a two-step process of an initial coordination of the thiol to the metal center followed by reductive elimination to form the *S*-aryl bond. This stands in contrast to other cysteine modification mechanisms that rely on displacement of an alkyl halide or 1,4-addition into a Michael acceptor. Our groups have reported the use of *P,N*-ligated Au(III) OACs for the *S*-arylation of cysteine (Fig. 1),[33–35] and recently, we have shown that stopped-flow/UV-vis spectroscopy is a powerful technique to characterize the rates of the two distinct elementary steps of the *S*-arylation. This allowed for the quantification of the bimolecular thiol

Department of Chemistry and Biochemistry and California NanoSystems Institute, University of California, Los Angeles, California, 90095-1569, USA. E-mail: spokoyny@chem.ucla.edu; houk@chem.ucla.edu; maynard@chem.ucla.edu

† Electronic supplementary information (ESI) available. See DOI: https://doi.org/10.1039/d4sc05920d

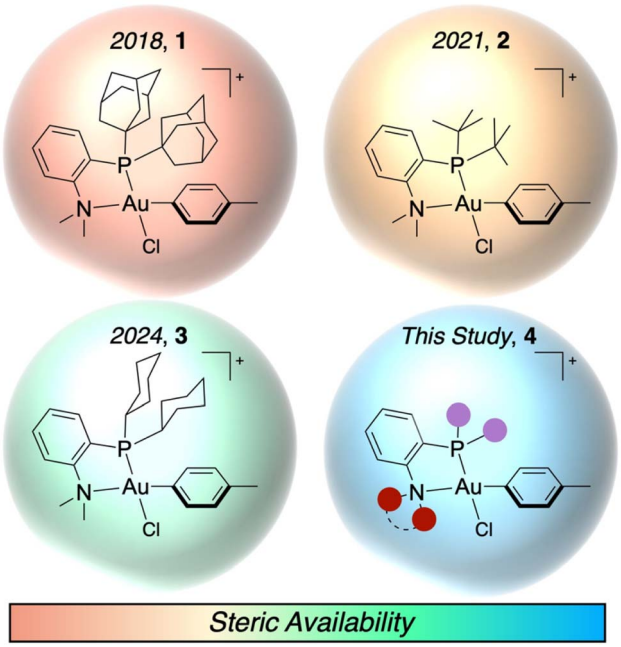

Fig. 1 *P,N*-ligated Au(III) complexes developed for rapid and selective cysteine *S*-arylation. Purple and red circles represent sites for modification on the ligand scaffold. Counterion not included for clarity.

coordination rate constant (k_{Co}) for *P,N*-ligated Au(III) OACs with di-1-adamantylphosphine (PAd_2) **1** and di-*tert*-butylphosphine (P^tBu_2) **2** *P*-substituents as 2460 and 4220 M^{-1} s^{-1}, respectively. The clear steric dependence on this coordination event led to the synthesis of a dicyclohexylphosphine-based (PCy_2) *P,N*-ligated Au(III) OAC reagent **3** with an unprecedented k_{Co} of 16 600 M^{-1} s^{-1}.[35]

Alternatively, by increasing the steric bulk of the aryl group, the coordination of the thiol to the Au(III) center was slowed down, which allowed for the chemoselective *S*-arylation of cysteine. By calculating the percent buried volume (% V_{Bur}) of the Au(III) OAC, a steric parameter was produced that could be used to predict the rate of coordination to the Au(III) center for both the ligand and aryl modifications. Herein, we demonstrate the extrapolation of % V_{Bur} as a screening metric for the expansion of Au(III) OACs for *S*-arylation. As the dialkylphosphine and amine could both be modified during the synthesis of the *P,N*-ligand, *in silico* screening was performed for eight dialkylphosphine substituents and five amine groups to examine their steric properties (Fig. 1, **4**). Additionally, the free energy of reaction (ΔG_{Rxn}) as well as the free energy of activation for the reductive elimination ($\Delta G^{\ddagger}_{RE}$) were calculated to examine the thermodynamics of each *P,N*-ligated Au(III) OAC. This allowed for the rapid screening of 13 different Au(III) OACs. Three of these novel *P,N*-ligated Au(III) OACs were synthesized, then their kinetics and efficiency as *S*-arylation reagents were determined. This led to the generation of k_{Co} up to 20 200 M^{-1} s^{-1}, improving upon the previously developed Au(III) OACs and demonstrating the computational and experimental synergy available in the investigation of metal-mediated bioconjugation reactions. These results also provide additional mechanistic insight into the coordination chemistry of Au(III) compounds.[36–40]

Results and discussion

Computational screening of *P,N*-Ligated Au(III) OACs

Previously, DFT calculations for the *S*-arylation of methanethiol were performed with NMe_2-containing *P,N*-ligated Au(III) phenyl OACs with PAd_2 (**5**), P^tBu_2 (**6**), and PCy_2 (**7**) *P*-substituents.[35] This reaction proceeds through a reversible coordination of the thiol to the Au(III) center of **SM**, generating **Int1**. Reductive elimination ($\mathbf{TS_{RE}}$) from **Int1** irreversibly forms the C(sp^2)–S bond (**Int2**), then product dissociation forms the free *S*-arylated product ($\mathbf{P_{Ar}}$) in addition to the Au(I) chloride starting material ($\mathbf{P_{Au}}$, Fig. 2A).[41] These calculations revealed that reagents **5–7** had a low $\Delta G^{\ddagger}_{RE}$ and a thermodynamically favorable ΔG_{Rxn}. Additionally, by calculating the % V_{Bur} of the Au(III) OAC (**SM**) of **5–7**, % V_{Bur} of 70.0, 69.8, and 67.1 were obtained, respectively.[42] This steric parameter is in agreement with the experimentally determined k_{Co} for each of these complexes wherein the more sterically available complexes (*i.e.* less % V_{Bur}) exhibited faster thiol coordination. We therefore hypothesized that the % V_{Bur} parameter could be used as a predictive metric for the rate of thiol coordination to the Au(III) center.

To further enhance this rate of coordination, we sought to screen smaller dialkylphosphines to provide more sterically available *P,N*-ligated Au(III) OACs using NMe_2 as the *N*-substituent. Accordingly, diisopropylphosphine-(P^iPr_2) (**8**) and dicyclopentylphosphine-based (PCp_2) (**9**) *P,N*-ligated Au(III) **SM** geometries were calculated at the ωB97X-D/6-311+G(d,p), SDD, CPCM(water)//B3LYP-D3/6-31G(d), LANL2DZ, CPCM(water) level of theory. Complexes **8** and **9** had % V_{Bur} of 66.8 and 66.5, respectively. These values are very similar to the NMe_2-PCy_2-ligated OAC **7**, so these ligands should affect a modest improvement on k_{Co}. For **8** and **9**, the comparable angles of the dialkylphosphine alkyl groups lead to similarly sized substituents compared to the cyclohexyl ring, which contributes to the small difference in % V_{Bur} compared to **7**. To this end, smaller ring sizes on the dialkylphosphine fragment of the *P,N*-ligand were examined to affect larger changes in % V_{Bur}. Dicyclobutylphosphine-($PCyb_2$) (**10**) and dicylopropylphosphine-based ($PCyp_2$) (**11**) *P,N*-ligated OACs were determined to have 65.6 and 63.2 % V_{Bur}, respectively. These values demonstrate that the smaller alkyl substituents induce more steric availability around the Au(III) center (Fig. 2B). To determine the lower limit of % V_{Bur} for these dialkylphosphine *P,N*-ligated Au(III) OACs, dimethylphosphine-based (PMe_2) *P,N*-ligated **SM** (**12**) was examined and found to have 61.6 % V_{Bur}.

Inspired by recent work developing bicyclo[1.1.1]pentyl- and bicyclo[1.1.0]butyl-containing phosphines that are more strained and consequently smaller compared to their cycloalkyl counterparts,[43,44] the % V_{Bur} for the di(bicyclo[1.1.1]pentyl) phosphine-($PBcp_2$) (**13**) and di(bicyclo[1.1.0]butyl)phosphine-based ($PBcb_2$) (**14**) *P,N*-ligated OACs were computed. Compound **13** had a % V_{Bur} of 65.5 while **14** had a % V_{Bur} of 63.5. These dialkylphosphines provide a significant decrease in % V_{Bur} compared to *P,N*-ligated **SM 9** (PCp_2) and **10** ($PCyb_2$), which

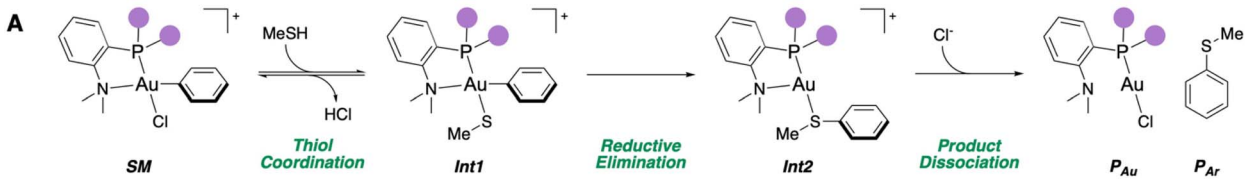

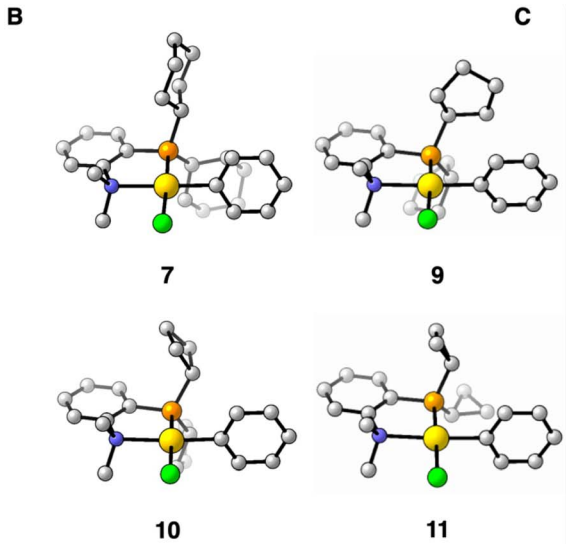

C

Diphosphine	*SM* %V_{Bur}	$\Delta G_{RE}^{\ddagger}$ (kcal mol^{-1})	ΔG_{Rxn} (kcal mol^{-1})
PAd_2[a] (**5**)	70.0	17.4	-23.8
P^tBu_2[a] (**6**)	69.8	17.9	-24.6
PCy_2[a] (**7**)	67.1	22.7	-20.0
P^iPr_2 (**8**)	66.8	22.7	-21.0
PCp_2 (**9**)	66.5	22.1	-22.9
$PCubane_2$ (**15**)	65.9	23.1	-21.3
$PCyb_2$ (**10**)	65.6	20.5	-22.5
$PBCp_2$ (**13**)	65.5	22.0	-22.0
$PBCb_2$ (**14**)	63.5	22.1	-23.6
$PCyp_2$ (**11**)	63.2	22.2	-24.3
PMe_2 (**12**)	61.6	24.8	-21.0

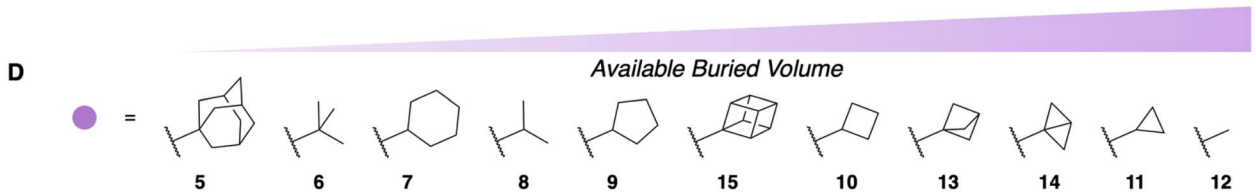

Fig. 2 (A) Proposed mechanism for the *S*-arylation of methanethiol mediated by Au(III) OACs. (B) **SM** geometries calculated for reagents **7**, **9**, **10**, and **11** at the ωB97X-D/6-311+G(d,p), SDD, CPCM(water)//B3LYP-D3/6-31G(d), LANL2DZ, CPCM(water) level of theory. (C) Table of % V_{Bur}, $\Delta G_{RE}^{\ddagger}$, and ΔG_{Rxn} for the different dialkylphosphine substituents examined. [a]These parameters were calculated previously.[35] (D) Schematic representation showing the dialkylphosphine variations in order of least to most available % V_{Bur}.

is in agreement with the additional strain in the bicyclic systems leading to smaller ring sizes and therefore less % V_{Bur}. The dicubylphosphine-based ($PCubane_2$) *P*,*N*-ligated **SM** (**15**) was also examined, which could be employed due to its similarity to **6** (P^tBu_2). Complex **15** had a % V_{Bur} of 65.9, indicating that formation of the cyclic scaffold does provide more steric availability to the **SM**. Taken together, these eight new Au(III) OACs (**8–15**) provide significant changes in % V_{Bur} compared to previously examined reagents **5–7** (Fig. 2D).

We previously determined that while the coordination to the Au(III) center is important, the subsequent, irreversible reductive elimination to form the C(sp^2)–S bond (**P_{Ar}**) remains a key step in the *S*-arylation.[35] Accordingly, the $\Delta G_{RE}^{\ddagger}$ and ΔG_{Rxn} were computed for each of the complexes. All of the reactions were calculated to be exergonic and irreversible. With the exception of the PMe_2 *P*-substituted OAC (**12**), the $\Delta G_{RE}^{\ddagger}$ values are reasonable to undergo sufficiently fast reductive elimination at 25 °C (20.5–23.1 kcal mol^{-1}), but the $\Delta G_{RE}^{\ddagger}$ of 24.8 kcal mol^{-1} for **12** likely prevents it from performing an efficacious reductive elimination at ambient temperature (Fig. 2C).

While prior work from our group has focused on modifying the dialkylphosphine component of the *P*,*N*-ligand, there has been research varying the amino fragment of these *P*,*N*-ligands in Pd catalysis, most notably to morpholine and piperidine.[45–49] Accordingly, these Au(III) complexes with morpholine (**16**) and piperidine (**17**) were calculated with a PAd_2 *P*-substituent (Fig. 3A), but there was a marginal difference in % V_{Bur} compared to the dimethylamino reagent (**5**, Fig. 3B). We hypothesized that by contracting the ring size, one could generate more sterically available Au(III) OACs. Pyrrolidine (**18**), azetidine (**19**), and aziridine (**20**) were consequently incorporated into the PAd_2-based *P*,*N*-ligated Au(III) complex and determined to have % V_{Bur} of 69.5, 68.6, and 66.7 (Fig. 3B–D), respectively. These results are in line with the dialkylphosphine calculations (Fig. 2) wherein the five-membered ring is similar to the six-membered ring, but significant changes are observed in the four- and three-membered rings. To ensure that these amine modifications did not have significant effects on the thermodynamics of the reaction, the $\Delta G_{RE}^{\ddagger}$ and ΔG_{Rxn} were computed for **16–20**. Each reaction was calculated to be

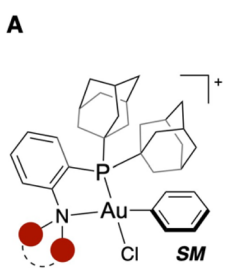

Available Buried Volume

B

Amine	*SM* %V_{Bur}	$\Delta G_{RE}^{\ddagger}$ (kcal mol^{-1})	ΔG_{Rxn} (kcal mol^{-1})
NMe_2[a] (**5**)	70.0	17.4	-23.8
Morpholine (**16**)	69.5	17.1	-33.8
Piperidine (**17**)	69.5	12.2	-33.3
Pyrrolidine (**18**)	69.5	17.5	-25.6
Azetidine (**19**)	68.6	18.8	-22.8
Aziridine (**20**)	66.7	18.5	-22.4

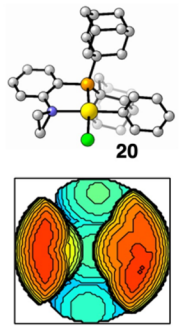

Fig. 3 (A) Generalized geometry for the Au(III) SM being modified. (B) Table of SM % V_{Bur}, $\Delta G_{RE}^{\ddagger}$, and ΔG_{Rxn} for the different amine substituents examined. [a]These parameters were calculated previously.[35] (C) SM geometry for reagent **20** calculated at the ωB97X-D/6-311+G(d,p), SDD, CPCM(water)//B3LYP-D3/6-31G(d), LANL2DZ, CPCM(water) level of theory. (D) Buried volume plot for the SM of **20**.

exergonic and irreversible with a low $\Delta G_{RE}^{\ddagger}$ (12.2–18.8 kcal-mol^{-1}) (Fig. 3B). Notably, the $\Delta G_{RE}^{\ddagger}$ for the piperidine-containing OAC (**16**) is significantly lower than the other complexes, potentially due to relaxation of the amine fragment from the twist-boat conformation in the *S*-coordinated **Int1** to the chair conformation in the transition state (see ESI† for details). This complex may warrant further examination to determine its ability to mediate other, more challenging reductive eliminations,[50] but the high % V_{Bur} indicates that it will likely not have a faster coordination than the other complexes examined herein.

Synthesis of *P*,*N*-ligands, Au(I) complexes, and Au(III) OACs

To validate these computational results, we sought to synthesize the compounds with both a lower % V_{Bur} than the NMe_2-PCy_2 ligated OAC (**7**) and a reasonable $\Delta G_{RE}^{\ddagger}$. Accordingly, the PCp_2-, $PCyb_2$-, and $PCyp_2$-based *P*,*N*-ligands with NMe_2 as the *N*-substituent were targeted due to their predicted rapid coordination and sufficiently fast reductive elimination. While the bicyclic systems **13** and **14** did have lower % V_{Bur} compared to their cyclic counterparts, they each had a similar % V_{Bur} to the more synthetically accessible $PCyb_2$- (**10**) and $PCyp_2$-based (**11**) systems. Due to this and their synthetic difficulty, **13** and **14** were not further examined. For the amine components, we wanted to synthesize the PAd_2 ligand with azetidine and aziridine as the amino substituent. However, the phenyl aziridine complex polymerizes in water,[51] which makes it an unsuitable reagent to perform bioconjugation reactions. We also wanted to examine if modifying both the *P*- and the *N*-substituents of the ligand simultaneously generated an additive effect of the two substitutions. To do this, the azetidine-PCy_2 complex was targeted.

The NMe_2-PCp_2 ligand **21** was synthesized by *in situ* formation of the aryl lithiate from 2-iodo-*N*,*N*-dimethylaniline and *n*-BuLi then substitution with the commercially available chlorodicyclopentylphosphine (see ESI† for details). Incomplete conversion to the desired *P*,*N*-ligand necessitated purification of the ligand by preparative high performance liquid chromatography (HPLC). Attempts to generate the NMe_2-$PCyb_2$ and NMe_2-$PCyp_2$ ligands relied on formation of the aryl lithiate and *in situ* generation of the chlorodialkylphosphine using phosphorus trichloride and the corresponding Grignard reagent. Purification of these reagents by preparative HPLC induced significant formation of the phosphine oxide, limiting the utility of these ligands. Other synthetic efforts to obtain these ligands involved formation of the phosphine oxide and subsequent reduction,[52] as well as attempts to generate 2-(dichlorophosphaneyl)-*N*,*N*-dimethylaniline,[53] which could then react with the cyclobutyl and cyclopropyl Grignard reagents. These routes provided low conversion to product and formation of multiply arylated byproducts, respectively.

However, the azetidine-PAd_2 ligand (**22**) and azetidine-PCy_2 ligand (**23**) could be readily accessed by Pd-catalyzed C(sp^2)–P bond formation from the corresponding *ortho*-halo-substituted aniline species and the dialkylphosphine in good isolated yield (80% and 63% yield, respectively). With *P*,*N*-ligands **21–23** isolated (Fig. 4A), the Au(I) complexes (**24–26**) were generated using $HAuCl_4 \cdot 3(H_2O)$ and 2,2′-thiodiethanol as a water-soluble variant of the commercially available Au(I)Cl(SMe_2) (Fig. 4B, see ESI† for details). The Au(III) OACs with a *p*-toluene aryl substituent (**27–29**) were synthesized using $AgSbF_6$ as a halide scavenger and 4-iodotoluene to generate a model compound for kinetic investigations (Fig. 4C, see ESI† for details).

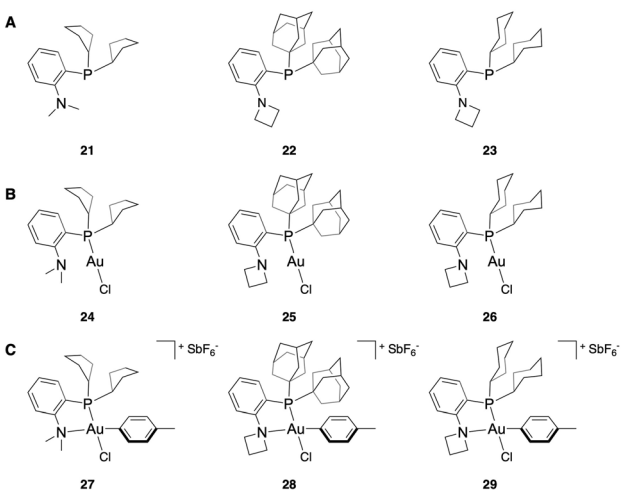

Fig. 4 Structures of *P*,*N*-ligands (A), Au(I) complexes (B), and Au(III) OACs (C) synthesized.

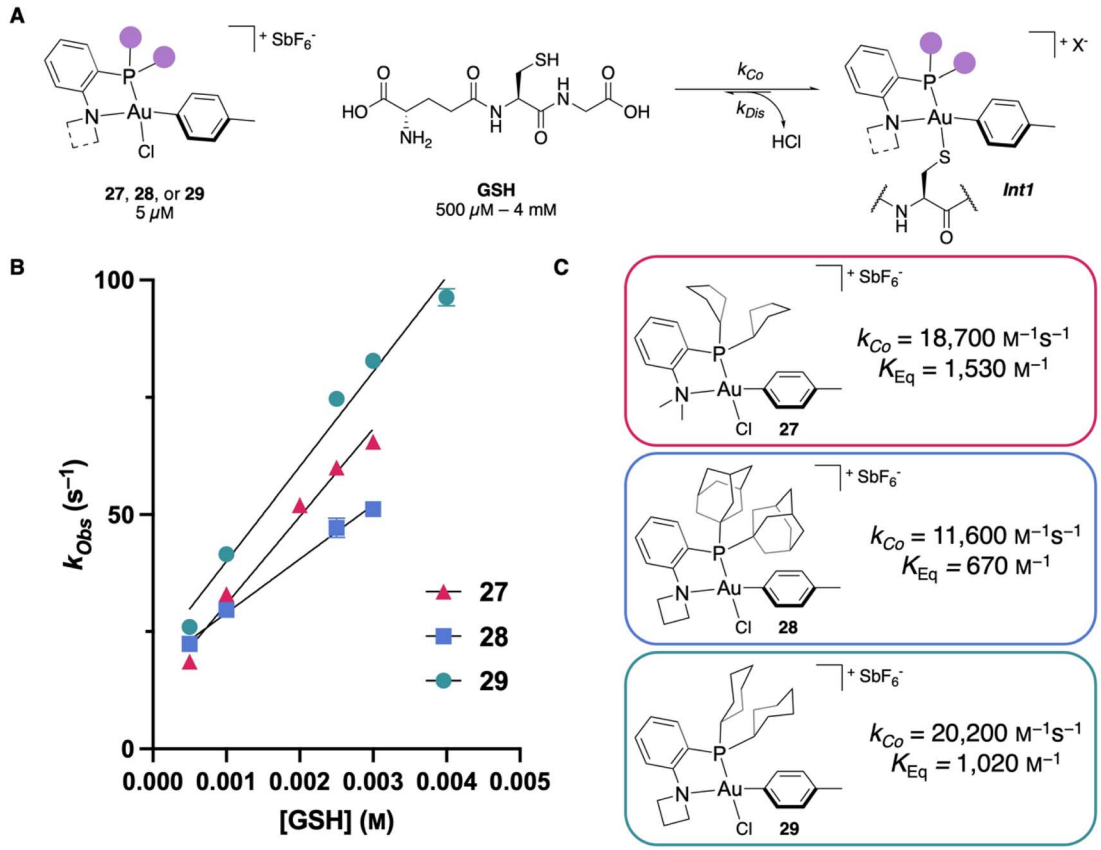

Fig. 5 (A) Generalized scheme for coordination monitoring from Au(III) OACs. X^- is used as a generalized counterion. Experiments were performed in 1 : 1 MeCN/100 mM Tris buffer at pH 7.4 and 20 °C. (B) Kinetic plots for coordination monitoring, $n = 5$ – some error bars are smaller than the markers. (C) Extracted k_{Co} and K_{Eq} for reagents **27**–**29**.

Thiol coordination rate monitoring

With the Au(III) OACs in hand, we wanted to test the kinetics of the thiol coordination to validate our computational predictions. To perform the coordination kinetics studies, stopped-flow/UV-vis spectroscopy experiments were performed at 5 μM of OAC with glutathione (**GSH**) as a model thiol under pseudo-first order

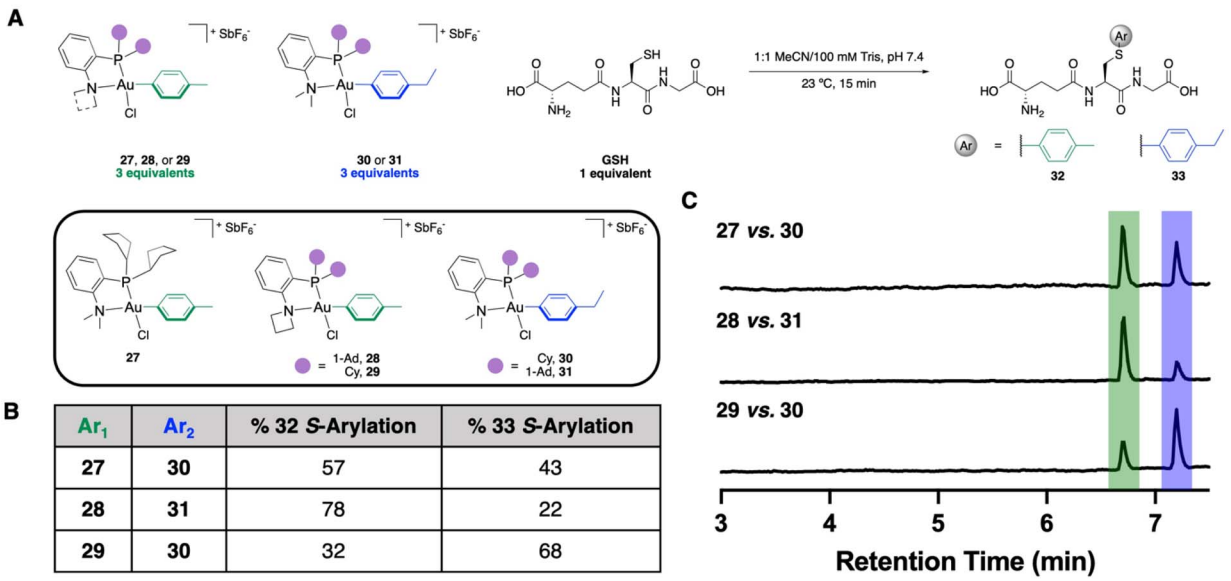

Ar_1	Ar_2	% 32 *S*-Arylation	% 33 *S*-Arylation
27	30	57	43
28	31	78	22
29	30	32	68

Fig. 6 (A) Generalized scheme and reagents used for the *S*-arylation competition experiments. (B) Results of the *S*-arylation competition experiments, $n = 3$. See ESI† for further details. (C) Total ion chromatogram traces from a representative replicate from each LC-MS competition experiment.

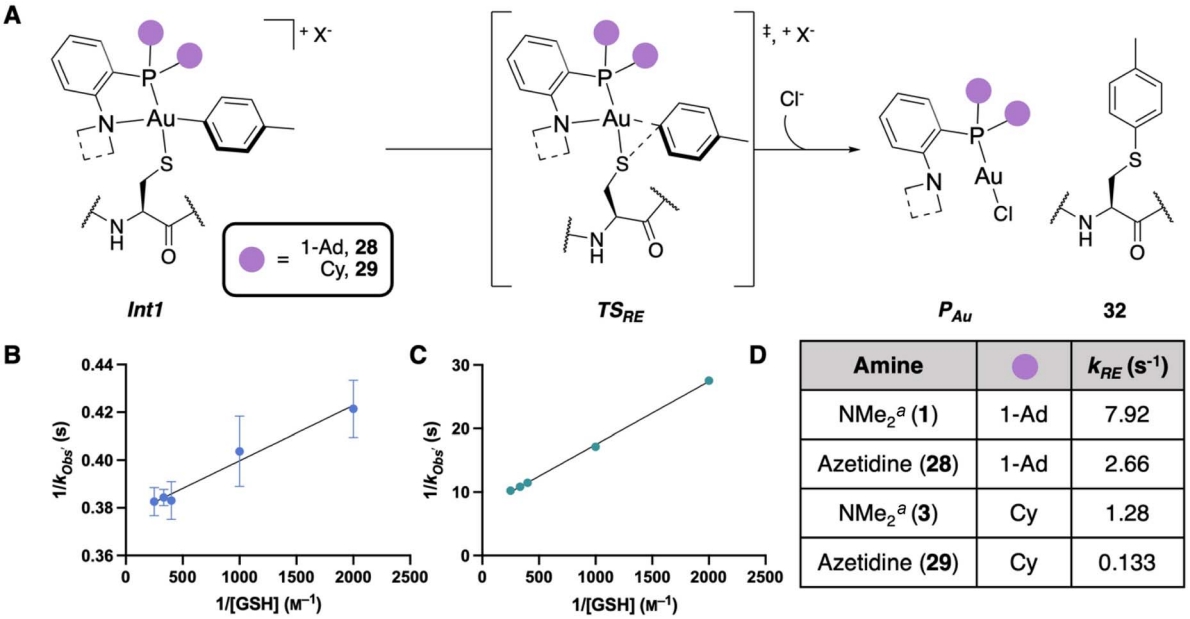

Amine		k_{RE} (s^{-1})
NMe_2[a] (**1**)	1-Ad	7.92
Azetidine (**28**)	1-Ad	2.66
NMe_2[a] (**3**)	Cy	1.28
Azetidine (**29**)	Cy	0.133

Fig. 7 (A) Generalized scheme for reductive elimination monitoring from **Int1**. X^- is used as a generalized counterion. Experiments were performed in 1 : 1 MeCN/100 mM Tris buffer at pH 7.4 and 20 °C. (B) Kinetic plot for the reductive elimination monitoring from **28**-**Int1**, $n = 5$. (C) Kinetic plot for the reductive elimination monitoring from **29**-**Int1**, $n = 3$ – some error bars are smaller than the markers. (D) k_{RE} comparison for the amine and dialkylphosphine modifications. [a]These parameters were determined previously.[35]

conditions (500 μM–4 mM of **GSH**) at pH 7.4 and 20 °C (Fig. 5A, see ESI† for details). By monitoring the absorbance, one can determine the formation of **Int1** and extrapolate the observed second-order rate constant, k_{Co}, from the experimentally observed rate constant (k_{Obs}). Examining **27**, a k_{Co} of 18 700 M^{-1} s^{-1} was calculated, which is faster than the NMe_2-PCy_2-ligated OAC **3** (16 600 M^{-1} s^{-1}). Also, the equilibrium of this complex is significantly shifted toward the S-coordinated intermediate (**Int1**) with a K_{Eq} (k_{Co}/k_{Dis}) of 1530 M^{-1} (Fig. 5B and C).

Next, rate measurements were performed for **28** to determine if modifying the amine fragment was another viable strategy to affect the k_{Co}. Kinetics experiments show that by utilizing the azetidine substituent, the k_{Co} increases to 11 600 M^{-1} s^{-1}, which is nearly a five-fold increase compared to the NMe_2-PAd_2-ligated reagent **1** (2460 M^{-1} s^{-1}). This increase in k_{Co} may also be attributed to less electron donation from azetidine compared to NMe_2, which would make the Au(III) center more electron poor and could accelerate the thiol coordination. By adding the P- and N-modifications together, we propose that **29** would provide the fastest k_{Co} reported. The studies were performed and a k_{Co} of 20 200 M^{-1} s^{-1} was observed for **29** (Fig. 5B and C), which represents a 25% increase in k_{Co} compared to **3** and is the fastest observed rate for S-coordination to an organometallic Au(III) compound to date. These results are all consistent with the % V_{Bur} calculations (Fig. 2C and 3B), validating the use of % V_{Bur} as a steric descriptor to predict the rate of bimolecular coordination for these Au(III) OACs.

S-Arylation competition experiments

With the k_{Co} determined for these three OACs, as well as the equilibria showing preferential thermodynamic formation of **Int1**, we next wanted to determine if the bimolecular coordination elementary step was still the selectivity-determining step in the reaction by performing *S*-arylation competition experiments. These experiments were performed by incubating one equivalent of **GSH** with three equivalents of two different OACs. These OACs vary by one methylene unit, which allows us to determine by liquid chromatography-mass spectrometry (LC-MS) which Au(III) reagent mediates the *S*-arylation more effectively (Fig. 6A). The NMe_2-PCy_2-(**30**) and NMe_2-PAd_2-ligated (**31**) Au(III) OACs with a *p*-ethylbenzene aryl substituent were prepared accordingly.

A competition experiment was performed between the NMe_2-PCp_2 (**27**) and NMe_2-PCy_2 (**30**) Au(III) OACs, which resulted in a 57 : 43 preference for the *p*-tolyl *S*-arylated product (**32**) over the *p*-ethylbenzene *S*-arylated product (**33**) (Fig. 6B and C). This preferential *S*-arylation from the NMe_2-PCp_2 OAC is in agreement with both the % V_{Bur} calculations as well as the k_{Co} obtained from stopped-flow kinetics. To examine the amine fragments, competition experiments were performed using the PAd_2-based *P*,*N*-ligated Au(III) OACs with azetidine (**28**) and dimethylamino (**31**) *N*-substitution. A 78 : 22 formation of **32** : **33** shows a preference for *S*-arylation from the azetidine-containing ligand (Fig. 6B and C), which is also in agreement with the % V_{Bur} calculations and the stopped-flow kinetics.

However, when the competition experiments were performed using the PCy_2-based *P*,*N*-ligated Au(III) OACs using the azetidine (**29**) and dimethylamino (**30**) *N*-substituents, a 32 : 68 ratio for **32** : **33** was observed (Fig. 6B and C). This indicates preferential *S*-arylation from the dimethylamino-containing ligand **30**. The % V_{Bur} calculations and the stopped-flow kinetics indicate that coordination is faster to **29**, but we hypothesize that the reductive elimination is slower, allowing

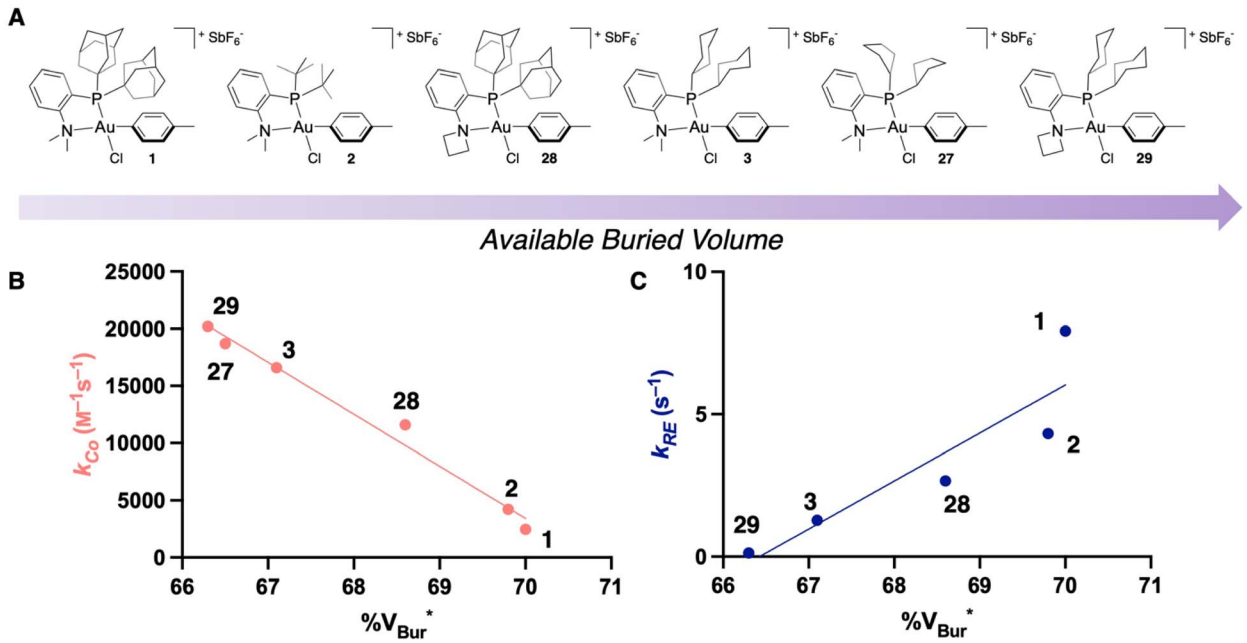

Fig. 8 (A) Ordering of the experimentally characterized Au(III) OACs from this and previous studies in order of least to most available % V_{Bur}.[35] (B) Plot of experimentally determined k_{Co} against % V_{Bur} for the Au(III) OACs shown in Fig. 8A. *% V_{Bur} is for the phenyl OAC and the counterion is not included. (C) Plot of experimentally determined k_{RE} against % V_{Bur} for the Au(III) OACs shown in Fig. 8A. *% V_{Bur} is for the phenyl OAC and the counterion is not included.

for a reversible coordination. This leads to a potential switch in the selectivity-determining step for this reaction and indicates that while the two ligand permutations are additive for the thiol coordination event, both elementary steps of the *S*-arylation need to be sufficiently fast to induce effective conjugation.

Reductive elimination rate monitoring

To examine the effects of the azetidine compounds on the reductive elimination, stopped-flow/UV-vis spectroscopy was performed using the conditions described *vide supra* (Fig. 7A, see ESI† for details). From **Int1** of **28**, a unimolecular rate constant was observed for the reductive elimination (k_{RE}) of 2.66 s^{-1} (Fig. 7B), which is approximately three times slower than k_{RE} of the NMe_2-PAd_2-ligated OAC **1** (Fig. 7D). This is also in line with the calculated $\Delta G^{\ddagger}_{RE}$ for the phenyl OACs (Fig. 3B). Profiling the reductive elimination from **Int1** of **29**, a k_{RE} of 0.133 s^{-1} was calculated (Fig. 7C), which is nearly ten times slower than the k_{RE} for the NMe_2-PCy_2-ligated OAC **3** (Fig. 7D). These results confirm the proposed switch in selectivity-determining step for **29** as observed in the competition experiments.

Altogether, this work demonstrates that % V_{Bur} can serve as a quickly calculated metric to screen the rate of bioconjugation to an Au(III) OAC, which will be valuable for the future screening of Au(III) and other metal complexes for bioconjugation. While the % V_{Bur} can be used to predict the rate of coordination to the Au(III) center, it can also be used to predict the rate of reductive elimination, though the trend is in the opposite direction (Fig. 8). These modifications that affect the steric bulk of the ligand may also modify the electronic properties of the complexes,[54–56] which can impact both the rate of coordination to the metal center as well as the rate of reductive elimination.[57–59] These factors should also be considered when designing new ligands for metal-catalyzed or metal-mediated transformations.

We propose that this workflow should be amenable to other metal-mediated *S*-arylation reactions and provide a rapid way to screen the efficacy of these reagents. This work also provides fundamental mechanistic insight into the elementary steps of Au(III) chemistry,[36,60–65] which is relatively understudied compared to Pd(II) and Pt(II) systems.

Conclusions

Thirteen Au(III) OACs were examined with eight different dialkylphosphines and five different amines *in silico* to determine their effects on both steps of the *S*-arylation reaction. Three novel Au(III) OACs were synthesized (**27**–**29**) and their bimolecular rate constants were determined to be between 11 600–20,200 M^{-1} s^{-1}. Finally, these OACs were examined in competition experiments to elucidate which of the two elementary steps of the *S*-arylation controls the selectivity, and a switch in the selectivity-determining step was confirmed experimentally for one of these reagents.

Data availability

All data are available free of charge in the ESI,† including experimental details, NMR spectra, characterization, kinetic data, and coordinates of computed structures. The raw data that support the findings of this study are available at **https://github.com/jtreacy01/Ultrafaster/**.

Author contributions

Joseph W. Treacy: conceptualization, computation, synthesis, formal analysis, writing – original draft. James A. R. Tilden: formal analysis, writing – original draft. Elaine Y. Chao: computation, formal analysis. Zihuan Fu: synthesis. Alexander M. Spokoyny: conceptualization, supervision, writing – review and editing, funding acquisition. K. N. Houk: supervision, writing – review and editing, funding acquisition. Heather D. Maynard: supervision, writing – review and editing, funding acquisition. All authors have given approval to the final version of the manuscript.

Conflicts of interest

The authors declare the following competing financial interest(s): A. M. S. and H. D. M. are co-inventors on several patent applications from UCLA associated with the Au(III) based bioconjugation technology.

Acknowledgements

This work was funded in part by the NSF (CHE-2404202, CHE-2003946, and CHE-2153972) and the NIH (R01DK127908). A. M. S. thanks NIGMS (R35GM124746) for funding. J. W. T. thanks UCLA Dissertation Year Fellowship for support. Z. F. thanks National Institute of Health Chemistry-Biology Interface Training Grant (T32GM136614) for support. NMR spectrometers are supported in part by the S10 program of the NIH Office of Research Infrastructure Programs under grant S10OD028644. The stopped-flow/UV-vis spectrometer was supported by the NIH (1S10OD023584). This work used computational and storage services associated with the Hoffman2 Shared Cluster provided by the UCLA Institute for Digital Research and Education's Research Technology Group.

References

1 S. B. Gunnoo and A. Madder, Chemical Protein Modification through Cysteine, *ChemBioChem*, 2016, **17**, 529–553.
2 J. M. Chalker, G. J. L. Bernardes, Y. A. Lin and B. G. Davis, Chemical Modification of Proteins at Cysteine: Opportunities in Chemistry and Biology, *Chem.–Asian J.*, 2009, **4**, 630–640.
3 O. Boutureira and G. J. L. Bernardes, Advances in Chemical Protein Modification, *Chem. Rev.*, 2015, **115**, 2174–2195.
4 A. D. Baldwin and K. L. Kiick, Tunable Degradation of Maleimide–Thiol Adducts in Reducing Environments, *Bioconjugate Chem.*, 2011, **22**, 1946–1953.
5 A. D. Baldwin and K. L. Kiick, Reversible maleimide–thiol adducts yield glutathione-sensitive poly(ethylene glycol)–heparin hydrogels, *Polym. Chem.*, 2013, **4**, 133–143.
6 E. H. Krenske, R. C. Petter and K. N. Houk, Kinetics and Thermodynamics of Reversible Thiol Additions to Mono- and Diactivated Michael Acceptors: Implications for the Design of Drugs That Bind Covalently to Cysteines, *J. Org. Chem.*, 2016, **81**, 11726–11733.
7 S. Krishnan, R. M. Miller, B. Tian, R. D. Mullins, M. P. Jacobson and J. Taunton, Design of Reversible, Cysteine-Targeted Michael Acceptors Guided by Kinetic and Computational Analysis, *J. Am. Chem. Soc.*, 2014, **136**, 12624–12630.
8 B. Shi and M. F. Greaney, Reversible Michael addition of thiols as a new tool for dynamic combinatorial chemistry, *Chem. Commun.*, 2005, 886–888.
9 R. Walther, M. Park, N. Ashman, M. Welch, J. S. Carroll and D. R. Spring, Tuneable thiol exchange linkers for traceless drug release applications in prodrugs and ADCs, *Chem. Commun.*, 2024, **60**, 7025–7028.
10 C. Zhang, E. V. Vinogradova, A. M. Spokoyny, S. L. Buchwald and B. L. Pentelute, Arylation Chemistry for Bioconjugation, *Angew. Chem., Int. Ed.*, 2019, **58**, 4810–4839.
11 N. C. Price, M. Cohn and R. H. Schirmer, Fluorescent and spin label probes of the environments of the sulfhydryl groups of porcine muscle adenylate kinase, *J. Biol. Chem.*, 1975, **250**, 644–652.
12 A. M. Spokoyny, Y. Zou, J. J. Ling, H. Yu, Y.-S. Lin and B. L. Pentelute, A Perfluoroaryl-Cysteine S_NAr Chemistry Approach to Unprotected Peptide Stapling, *J. Am. Chem. Soc.*, 2013, **135**, 5946–5949.
13 C. Zhang, M. Welborn, T. Zhu, N. J. Yang, M. S. Santos, T. Van Voorhis and B. L. Pentelute, π-Clamp-mediated cysteine conjugation, *Nat. Chem.*, 2016, **8**, 120–128.
14 R. J. Taylor, M. Aguilar Rangel, M. B. Geeson, P. Sormanni, M. Vendruscolo and G. J. L. Bernardes, π-Clamp-Mediated Homo- and Heterodimerization of Single-Domain Antibodies *via* Site-Specific Homobifunctional Conjugation, *J. Am. Chem. Soc.*, 2022, **144**, 13026–13031.
15 H. F. Motiwala, Y. H. Kuo, B. L. Stinger, B. A. Palfey and B. R. Martin, Tunable Heteroaromatic Sulfones Enhance in-Cell Cysteine Profiling, *J. Am. Chem. Soc.*, 2020, **142**, 1801–1810.
16 K. C. Tang, S. M. Maddox, K. M. Backus and M. Raj, Tunable heteroaromatic azoline thioethers (HATs) for cysteine profiling, *Chem. Sci.*, 2022, **13**, 763–774.
17 B. M. Lipka, V. M. Betti, D. S. Honeycutt, D. L. Zelmanovich, M. Adamczyk, R. Wu, H. S. Blume, C. A. Mendina, J. M. Goldberg and F. Wang, Rapid Electrophilic Cysteine Arylation with Pyridinium Salts, *Bioconjugate Chem.*, 2022, **33**, 2189–2196.
18 B. M. Lipka, D. S. Honeycutt, G. M. Bassett, T. N. Kowal, M. Adamczyk, Z. C. Cartnick, V. M. Betti, J. M. Goldberg and F. Wang, Ultra-rapid Electrophilic Cysteine Arylation, *J. Am. Chem. Soc.*, 2023, **145**, 23427–23432.
19 C. Wan, Y. Zhang, J. Wang, Y. Xing, D. Yang, Q. Luo, J. Liu, Y. Ye, Z. Liu, F. Yin, R. Wang and Z. Li, Traceless Peptide and Protein Modification *via* Rational Tuning of Pyridiniums, *J. Am. Chem. Soc.*, 2024, **146**, 2624–2633.
20 E. V. Vinogradova, C. Zhang, A. M. Spokoyny, B. L. Pentelute and S. L. Buchwald, Organometallic palladium reagents for cysteine bioconjugation, *Nature*, 2015, **526**, 687–691.
21 J. A. R. Tilden, A. T. Lubben, S. B. Reeksting, G. Kociok-Köhn and C. G. Frost, Pd(II)-Mediated C−H Activation for Cysteine Bioconjugation, *Chem.–Eur. J.*, 2022, **28**, e202104385.

22 S. Gukathasan, S. Parkin, E. P. Black and S. G. Awuah, Tuning Cyclometalated Gold(III) for Cysteine Arylation and Ligand-Directed Bioconjugation, *Inorg. Chem.*, 2021, **60**, 14582–14593.
23 K. K.-Y. Kung, H.-M. Ko, J.-F. Cui, H.-C. Chong, Y.-C. Leung and M.-K. Wong, Cyclometalated gold(III) complexes for chemoselective cysteine modification *via* ligand controlled C–S bond-forming reductive elimination, *Chem. Commun.*, 2014, **50**, 11899–11902.
24 M. N. Wenzel, R. Bonsignore, S. R. Thomas, D. Bourissou, G. Barone and A. Casini, Cyclometalated Au-III Complexes for Cysteine Arylation in Zinc Finger Protein Domains: towards Controlled Reductive Elimination, *Chem.–Eur. J.*, 2019, **25**, 7628–7634.
25 G. E. Mudd, S. J. Stanway, D. R. Witty, A. Thomas, S. Baldo, A. D. Bond, P. Beswick and A. Highton, Gold-Mediated Multiple Cysteine Arylation for the Construction of Highly Constrained Bicycle Peptides, *Bioconjugate Chem.*, 2022, **33**, 1441–1445.
26 K. Hanaya, J. Ohata, M. K. Miller, A. E. Mangubat-Medina, M. J. Swierczynski, D. C. Yang, R. M. Rosenthal, B. V. Popp and Z. T. Ball, Rapid nickel(II)-promoted cysteine *S*-arylation with arylboronic acids, *Chem. Commun.*, 2019, **55**, 2841–2844.
27 L.-Z. Qin, H. Sun, X. Duan, S.-S. Zhu, J. Liu, M.-Y. Wu, X. Yuan, J.-K. Qiu and K. Guo, Visible-light-induced nickel-catalyzed selective S-arylation of peptides by exogenous-photosensitizer-free photocatalysis, *Cell Rep. Phys. Sci.*, 2023, **4**, 101292.
28 V. Bacauanu, Z. N. Merz, Z. L. Hua and S. B. Lang, Nickel-Catalyzed Antibody Bioconjugation, *J. Am. Chem. Soc.*, 2023, **145**, 25842–25849.
29 X. Chu, L. H. Shen, B. Li, P. Yang, C. Z. Du, X. Y. Wang, G. He, S. Messaoudi and G. Chen, Construction of Peptide Macrocycles *via* Palladium-Catalyzed Multiple S-Arylation: An Effective Strategy to Expand the Structural Diversity of Cross-Linkers, *Org. Lett.*, 2021, **23**, 8001–8006.
30 P. Yang, X. Wang, B. Li, Y. Yang, J. Yue, Y. Suo, H. Tong, G. He, X. Lu and G. Chen, Streamlined construction of peptide macrocycles *via* palladium-catalyzed intramolecular *S*-arylation in solution and on DNA, *Chem. Sci.*, 2021, **12**, 5804–5810.
31 E. V. Vinogradova, Organometallic chemical biology: an organometallic approach to bioconjugation, *Pure Appl. Chem.*, 2017, **89**, 1619–1640.
32 H. R. Montgomery, A. M. Spokoyny and H. D. Maynard, Organometallic Oxidative Addition Complexes for *S*-Arylation of Free Cysteines, *Bioconjugate Chem.*, 2024, **35**, 883–889.
33 M. S. Messina, J. M. Stauber, M. A. Waddington, A. L. Rheingold, H. D. Maynard and A. M. Spokoyny, Organometallic Gold(III) Reagents for Cysteine Arylation, *J. Am. Chem. Soc.*, 2018, **140**, 7065–7069.
34 J. M. Stauber, A. L. Rheingold and A. M. Spokoyny, Gold(III) Aryl Complexes as Reagents for Constructing Hybrid Peptide-Based Assemblies *via* Cysteine *S*-Arylation, *Inorg. Chem.*, 2021, **60**, 5054–5062.
35 E. A. Doud, J. A. R. Tilden, J. W. Treacy, E. Y. Chao, H. R. Montgomery, G. E. Kunkel, E. J. Olivares, N. Adhami, T. A. Kerr, Y. Chen, A. L. Rheingold, J. A. Loo, C. G. Frost, K. N. Houk, H. D. Maynard and A. M. Spokoyny, Ultrafast Au(III)-Mediated Arylation of Cysteine, *J. Am. Chem. Soc.*, 2024, **146**, 12365–12374.
36 L. Rocchigiani and M. Bochmann, Recent Advances in Gold(III) Chemistry: Structure, Bonding, Reactivity, and Role in Homogeneous Catalysis, *Chem. Rev.*, 2021, **121**, 8364–8451.
37 M. S. M. Holmsen, A. Nova and M. Tilset, Cyclometalated (N,C) Au(III) Complexes: The Impact of Trans Effects on Their Synthesis, Structure, and Reactivity, *Acc. Chem. Res.*, 2023, **56**, 3654–3664.
38 K. Muratov, E. Zaripov, M. V. Berezovski and F. Gagosz, DFT-Enabled Development of Hemilabile (P^N) Ligands for Gold(I/III) RedOx Catalysis: Application to the Thiotosylation of Aryl Iodides, *J. Am. Chem. Soc.*, 2024, **146**, 3660–3674.
39 A. Genoux, M. Biedrzycki, E. Merino, E. Rivera-Chao, A. Linden and C. Nevado, Synthesis and Characterization of Bidentate (P^N)Gold(III) Fluoride Complexes: Reactivity Platforms for Reductive Elimination Studies, *Angew. Chem., Int. Ed.*, 2021, **60**, 4164–4168.
40 J. Martín, E. Gómez-Bengoa, A. Genoux and C. Nevado, Synthesis of Cyclometalated Gold(III) Complexes *via* Catalytic Rhodium to Gold(III) Transmetalation, *Angew. Chem., Int. Ed.*, 2022, **61**, e202116755.
41 S.-L. Zhang and J.-J. Dong, Mechanism and chemoselectivity origins of bioconjugation of cysteine with Au(III)-aryl reagents, *Org. Biomol. Chem.*, 2019, **17**, 1245–1253.
42 L. Falivene, Z. Cao, A. Petta, L. Serra, A. Poater, R. Oliva, V. Scarano and L. Cavallo, Towards the online computer-aided design of catalytic pockets, *Nat. Chem.*, 2019, **11**, 872–879.
43 G. L. Perry and N. D. Schley, Tris(bicyclo[1.1.1]pentyl) phosphine: An Exceptionally Small Tri-*tert*-alkylphosphine and Its Bis-Ligated Pd(0) Complex, *J. Am. Chem. Soc.*, 2023, **145**, 7005–7010.
44 G. L. Perry and N. D. Schley, Bis(bicyclo[1.1.1]pentyl) chlorophosphine as a Precursor for the Preparation of Bis(bicyclo[1.1.1]pentyl)phosphines, *Org. Lett.*, 2024, **26**, 6071–6075.
45 S. M. Crawford, C. A. Wheaton, V. Mishra and M. Stradiotto, Probing the effect of donor-fragment substitution in Mor-DalPhos on palladium-catalyzed C–N and C–C cross-coupling reactivity, *Can. J. Chem.*, 2018, **96**, 578–586.
46 M. A. MacLean, C. A. Wheaton and M. Stradiotto, Developing backbone-modified Mor-DalPhos ligand variants for use in palladium-catalyzed C–N and C–C cross-coupling, *Can. J. Chem.*, 2018, **96**, 712–721.
47 B. J. Tardiff, R. McDonald, M. J. Ferguson and M. Stradiotto, Rational and Predictable Chemoselective Synthesis of Oligoamines *via* Buchwald–Hartwig Amination of (Hetero) Aryl Chlorides Employing Mor-DalPhos, *J. Org. Chem.*, 2012, **77**, 1056–1071.

48 P. G. Alsabeh, R. J. Lundgren, R. McDonald, C. C. C. Johansson Seechurn, T. J. Colacot and M. Stradiotto, An Examination of the Palladium/Mor-DalPhos Catalyst System in the Context of Selective Ammonia Monoarylation at Room Temperature, *Chem.–Eur. J.*, 2013, **19**, 2131–2141.
49 R. Lundgren, K. Hesp and M. Stradiotto, Design of New 'DalPhos' P,N-Ligands: Applications in Transition-Metal Catalysis, *Synlett*, 2011, **2011**, 2443–2458.
50 A. J. Mallek, B. L. Pentelute and S. L. Buchwald, Selective N-Arylation of *p* -Aminophenylalanine in Unprotected Peptides with Organometallic Palladium Reagents, *Angew. Chem., Int. Ed.*, 2021, **60**, 16928–16931.
51 H. W. Heine, B. L. Kapur, J. L. Bove, R. W. Greiner, K. H. Klinger and C. Mitch, The Synthesis of Some N-Arylethylenimines, *J. Am. Chem. Soc.*, 1954, **76**, 2503.
52 Y. Li, L.-Q. Lu, S. Das, S. Pisiewicz, K. Junge and M. Beller, Highly Chemoselective Metal-Free Reduction of Phosphine Oxides to Phosphines, *J. Am. Chem. Soc.*, 2012, **134**, 18325–18329.
53 J. W. M. MacMillan, R. T. McGuire, A. M. McMahon, T. S. Anderson, K. N. Robertson and M. Stradiotto, DalPhos on Demand: Facile Ligand Generation Enables New Ligand Discovery and Expedient Catalyst Screening, *ACS Catal.*, 2024, **14**, 4074–4081.
54 C. A. Tolman, Steric effects of phosphorus ligands in organometallic chemistry and homogeneous catalysis, *Chem. Rev.*, 1977, **77**, 313–348.
55 D. J. Durand and N. Fey, Computational Ligand Descriptors for Catalyst Design, *Chem. Rev.*, 2019, **119**, 6561–6594.
56 T. Gensch, G. dos Passos Gomes, P. Friederich, E. Peters, T. Gaudin, R. Pollice, K. Jorner, A. Nigam, M. Lindner-D'Addario, M. S. Sigman and A. Aspuru-Guzik, A Comprehensive Discovery Platform for Organophosphorus Ligands for Catalysis, *J. Am. Chem. Soc.*, 2022, **144**, 1205–1217.
57 J. F. Hartwig, Electronic Effects on Reductive Elimination To Form Carbon−Carbon and Carbon−Heteroatom Bonds from Palladium(II) Complexes, *Inorg. Chem.*, 2007, **46**, 1936–1947.
58 R. Martin and S. L. Buchwald, Palladium-Catalyzed Suzuki−Miyaura Cross-Coupling Reactions Employing Dialkylbiaryl Phosphine Ligands, *Acc. Chem. Res.*, 2008, **41**, 1461–1473.
59 J. W. Treacy, E. Y. Chao, G. E. Kunkel, T. Louis-Goff, J. A. R. Tilden, A. M. Spokoyny, H. D. Maynard and K. N. Houk, Electronic Effects of Bidentate *P,N* -Ligands on the Elementary Steps of Au(I)/Au(III) Reactions Relevant to Cross-Coupling Chemistry, *Org. Lett.*, 2024, **26**, 10875–10879.
60 M. S. Winston, W. J. Wolf and F. D. Toste, Halide-Dependent Mechanisms of Reductive Elimination from Gold(III), *J. Am. Chem. Soc.*, 2015, **137**, 7921–7928.
61 A. Casini, In My Element : Gold, *Chem.–Eur. J.*, 2019, **25**, 12234.
62 M. J. Harper, C. J. Arthur, J. Crosby, E. J. Emmett, R. L. Falconer, A. J. Fensham-Smith, P. J. Gates, T. Leman, J. E. McGrady, J. F. Bower and C. A. Russell, Oxidative Addition, Transmetalation, and Reductive Elimination at a 2,2′-Bipyridyl-Ligated Gold Center, *J. Am. Chem. Soc.*, 2018, **140**, 4440–4445.
63 D. Vesseur, S. Li, S. Mallet-Ladeira, K. Miqueu and D. Bourissou, Ligand-Enabled Oxidative Fluorination of Gold(I) and Light-Induced Aryl–F Coupling at Gold(III), *J. Am. Chem. Soc.*, 2024, **146**, 11352–11363.
64 C. C. Chintawar, V. W. Bhoyare, M. V. Mane and N. T. Patil, Enantioselective Au(I)/Au(III) Redox Catalysis Enabled by Chiral (P,N)-Ligands, *J. Am. Chem. Soc.*, 2022, **144**, 7089–7095.
65 A. Portugués, M. Á. Martínez-Nortes, D. Bautista, P. González-Herrero and J. Gil-Rubio, Reductive Elimination Reactions in Gold(III) Complexes Leading to C(sp^3)–X (X = C, N, P, O, Halogen) Bond Formation: Inner-Sphere *vs.* S_N2 Pathways, *Inorg. Chem.*, 2023, **62**, 1708–1718.